aerospace

MDPI

Article

Benefits from Thin-Ply Composite Materials in Aircraft Wing Structures

Lennart Lobitz [1,2,*], Christian Bülow [1,3], Sebastian Heimbs [1,2] and Peter Horst [1,2]

[1] Cluster of Excellence SE^{2}A—Sustainable and Energy-Efficient Aviation, TU Braunschweig, 38108 Braunschweig, Germany; christian.buelow@dlr.de (C.B.); s.heimbs@tu-braunschweig.de (S.H.); p.horst@tu-braunschweig.de (P.H.)
[2] Institute of Aircraft Design and Lightweight Structures (IFL), TU Braunschweig, 38108 Braunschweig, Germany
[3] Institute of Lightweight Systems, German Aerospace Center (DLR), 21684 Stade, Germany
* Correspondence: l.lobitz@tu-braunschweig.de; Tel.: +49-531-391-9957

Abstract

Previous research shows that thin-ply composite materials offer superior static and fatigue characteristics to standard laminates used in aviation. Therefore, they are expected to be capable of significantly contributing to a mass reduction needed to improve the energy-efficiency of future aircraft. However, so far, thin-ply composites have only been employed in special applications. Quantitative full-scale assessments of the benefits on the level of global aircraft structures are missing. This study employs a parametric, finite element-based tool chain with a fully-stressed design methodology to investigate potential benefits from the use of thin plies, which may result from increased strength, an extended design freedom and stability considerations, in a generic wing structure of a conceptual medium-range aircraft in order to reduce this research gap. The methodology is validated using an academic test case. Naturally, mass reductions from strength enhancements are limited by buckling constraints in thin-walled structures. However, for the wing examined in this study, an increase in strength of 10% still yields up to a 7.9% reduction in global wing mass, while an increase of 20% results in mass savings of up to 13.4%. The use of thin-ply composites may allow for reducing minimum wall thickness constraints. Associated mass savings of up to 3.1% found in this study on global wing level when alleviating the requirement from 2.4 mm to 1.2 mm are, however, restricted to rib mass and may better be achieved by different means such as topology optimisation. In contrast, mass penalties from the application of a simplified manufacturing constraint are reduced significantly from beyond 10% on global wing level for plies with a thickness of 0.175 mm to approximately 1.5% with a ply thickness of 0.05 mm.

Keywords: thin-ply; aircraft structures; composite structures; wing design

Academic Editors: Morteza Abouhamzeh and Bosko Rasuo

Received: 15 September 2025
Revised: 26 November 2025
Accepted: 2 December 2025
Published: 3 December 2025

Citation: Lobitz, L.; Bülow, C.; Heimbs, S.; Horst, P. Benefits from Thin-Ply Composite Materials in Aircraft Wing Structures. *Aerospace* **2025**, *12*, 1078. https://doi.org/10.3390/aerospace12121078

1. Introduction

Several new methods of energy storage and transformation are currently being investigated to reduce emissions of future aircraft. A major concern for both alternative fuels and electric propulsion is the energy density, in terms of weight and volume. In the German Cluster of Excellence for Sustainable and Energy-Efficient Aviation (SE^{2}A), complex approaches are pursued to overcome these shortcomings, ranging, e.g., from drastic drag reduction via hybrid laminar flow control to mass reduction through load alleviation [1–3].

Apart from these strategies, there obviously exists the more direct way of reducing the structural weight by employing novel lightweight material variants such as thin-ply composites, which in general can be defined as laminates with a ply thickness of less than 0.1 mm [4].

Beneficial effects of the structural–mechanical behaviour of thin-ply laminates were first reported by Sasayama [5]. Based on a spreading technique developed by Kawabe [6], Sihn et al. [7,8] further examined the properties of laminates manufactured from thin-ply prepreg. In the following years, other authors [9–15] made important contributions and analysed thin plies and their special properties in detail. An overview of the topic and the most important literature is given in the reviews of Arteiro [16] and Galos [4]. The in situ effect inherent to thin-ply laminates provides an explanation for the improved properties compared to laminates with thicker layers [11]. It implies that in laminates with thinner plies, transverse matrix cracks and delaminations are increasingly suppressed until a critical ply thickness is reached, below which such failure modes do not occur before final failure. This leads to a quasi-brittle failure mode with no sign of damage before final failure. In contrast, thicker plies fail in a progressive manner with transverse crack and delamination propagation up to final failure [11]. The in-situ effect is observed in the transverse tensile and compressive strength [17], as well as in the shear strength [18]. It requires adjacent plies to be orientated in distinct directions.

Table 1 presents a quantitave comparison of different mechanical properties in relation to layer thickness. A quite notable effect of the use of thin plies is found for the tensile strength in static tension (see Table 1a). Sihn et al. [8], for instance, compared quasi-isotropic (QI) laminates with a layer thickness of 0.04 mm and 0.2 mm, respectively, and found an increase in tensile strength of the thin-ply specimen of 10%. Table 1a clearly demonstrates that all referenced studies report a significant enhancement in tensile strength. Variations in the extent of the improvements, which are attributed to the in-situ effect [11], may be explained by differences both in the materials employed and the ply thickness compared. There is also a remarkable difference in the first ply failure behaviour between standard and thin plies in the results obtained by Amacher et al. [11]: while the ultimate strength is increased by a factor of 1.4, the stress at the damage initiation point even increases by a factor of 3.3 for thin plies. This may also be explained by the suppression of transverse cracks and delamination. In addition to the improvement in tensile strength, thin plies also enhance the static compressive strength of unnotched specimens as shown in Table 1b. The data from various sources consistently indicate significant increases in compressive strength in the range of 16% to 36%.

Nevertheless, thin plies do not enhance every strength metric. Table 1c shows the various results of studies that examined the open hole tension (OHT) strength of thin ply composites, which is reduced in comparison to thicker plies. The detected decrease in the thin-ply specimens ranges from −10% to −28%. It is attributed to the suppression of transverse cracks, which relax the stress around the hole and lead to a local stress redistribution when using specimens with higher ply thickness. Due to the absence of this stress redistribution, thin-ply composites fail in a premature, brittle failure mechanism [8,11]. However, the stress at the damage initiation point is still higher for the thin-ply composites, e.g., 38% in the results of Amacher et al. [11]. Therefore, the use of thin-ply composites may be beneficial in cases where the criteria is to avoid any damage. In contrast to OHT, the open hole compression properties (OHC) are improved again. Table 1d shows the results of different studies with significantly enhanced OHC strength in the range of 8% to 18%. Arteiro et al. [17] attribute this positive thin-ply effect to the failure mechanism of OHC specimens, which starts with fibre kinking and delamination around the hole. Due to the suppression of transverse cracks and delamination thin-ply laminates show a higher OHC strength.

Table 1. Literature results on the influence of thin-ply usage. Thin plies and Reference characterise the materials used for comparison, and Δ gives the difference in the respective performance metric.

	Layup	Thin Plies	Reference	Δ/%	Author
(**a**) Tensile strength	QI	0.04 mm	0.2 mm	10	Sihn et al. [8]
	QI	75 g/m^2	145 g/m^2	20	Yokozeki et al. [9]
	QI	0.06 mm	0.125 mm	9	Moon et al. [19]
	QI	30 g/m^2	300 g/m^2	13	Amacher et al. [11]
	QI	30 g/m^2	190 g/m^2	32	Lovejoy et al. [20]
(**b**) Compressive strength	QI	0.045 mm	0.136 mm	28	Kawabe et al. [21]
	QI	75 g/m^2	145 g/m^2	16	Yokozeki et al. [9]
	UD	30 g/m^2	100 g/m^2	21	Amacher et al. [11]
	QI	30 g/m^2	190 g/m^2	36	Lovejoy et al. [20]
(**c**) Open hole tension strength	QI	0.04 mm	0.2 mm	−10	Sihn et al. [8]
	QI	30 g/m^2	150 g/m^2	−25	Amacher et al. [11]
	QI	30 g/m^2	300 g/m^2	−30	Amacher et al. [11]
	QI	30 g/m^2	300 g/m^2	−28	Masania et al. [22]
	QI	20 g/m^2	125 g/m^2	−20	Huang et al. [23]
	QI	54 g/m^2	125 g/m^2	−10	Huang et al. [23]
(**d**) Open hole compression strength	QI	75 g/m^2	145 g/m^2	9	Yokozeki et al. [9]
	QI	30 g/m^2	150 g/m^2	11	Amacher et al. [11]
	QI	30 g/m^2	300 g/m^2	18	Amacher et al. [11]
	QI	30 g/m^2	190 g/m^2	8	Lovejoy et al. [20]

In addition to the considerations regarding strength, thin-ply composites offer an increased design freedom compared to standard aerospace materials. Considering a laminate with a thickness of 1 mm, it is possible to use eight layers with a cured thickness of 0.125 mm, but up to 25 layers with a thickness of 0.04 mm. By applying typical design guidelines such as a quasi-isotropic and symmetrical stacking, the resulting layup with eight layers is already very limited in design. In contrast, 25 layers allow it to fulfil the restrictions and additionally use other directions like 22.5° or 67.5°, enabling a smoother stiffness change and therefore less interlaminar stresses. Even a load path-optimised design is possible if no quasi-isotropic stacking is prescribed. The application of thin-ply laminates may significantly reduce the minimum wall thickness required for quasi-isotropic layups in low-stress regions. In addition, a further improvement to be gained is the fact that thickness variations may be adjusted in a much smoother way than for usual material. A symmetric and balanced laminate with a ply thickness of 0.125 mm e.g., results in steps of 1.0 mm, while it is only 0.4 mm for a thin-ply laminate with a ply-thickness of 0.05 mm.

A less obvious potential benefit concerns buckling stability. Upper wing covers are usually sized by buckling requirements to a large extent. This paper makes use of the no local buckling criterion up to limit load, as it is mostly part of the sizing process for carbon fibre-reinforced polymer (CFRP) structures in transport aircraft certification. The idea behind advantages from the use of thin-ply material is the following: initial buckling of a composite plate made of unidirectional layers is governed by the differential equation

$$D_{11}\frac{\partial^4 w}{\partial x^4} + 4D_{16}\frac{\partial^4 w}{\partial x^3 \partial y} + 2(D_{12}+2D_{66})\frac{\partial^4 w}{\partial x^2 \partial y^2} + 4D_{26}\frac{\partial^4 w}{\partial x \partial y^3} + D_{22}\frac{\partial^4 w}{\partial y^4} = n_x\frac{\partial^2 w}{\partial x^2} + 2\,n_{xy}\frac{\partial^2 w}{\partial x \partial y} + n_y\frac{\partial^2 w}{\partial y^2} \quad (1)$$

where $D_{\alpha\beta}$ are the elements of the bending stiffness matrix D in the ABD matrix and $n_{\alpha\beta}$ are the section forces in the directions. It is well known that the elements D_{16} and D_{26} have a detrimental effect on the buckling strength, in case they are different from zero. For unidirectional layers, as they are used in most prepreg laminates, it is not possible to reach $D_{16} = D_{26} = 0$ even in case of a balanced and symmetric layup, since the $\pm\theta$

layers (with $\theta \neq 0°$ or 90°) cannot have the same distance from the neutral plane. Thin plies allow to reduce this difference in distance from the neutral plane essentially, improving the buckling performance.

To date, there have been some employments of thin-ply composites in aerospace applications. One of the first examples is the use of Oxeon spread tow fabric in the manufacturing of the ultra light aircraft Shark Aero UL [24], resulting in fuselage weight savings of 38% with the use of 80 g/m^2 fabric. Amacher et al. [25] examine the usage of thin-ply prepreg in a rear tail boom mount of a helicopter. By using thin plies and changing the fibre type to a high-modulus fibre, a weight reduction of 15% is achieved while maintaining the same mechanical performance. Amacher et al. [26] describe the use of different thin plies in the spar box of Solar Impulse ranging from 100 g/m^2 to 25 g/m^2. Solar Impulse 2 is the first solar-powered fixed-wing aircraft to circumnavigate the world. Yamashita et al. [27,28] examine lightning strike properties of thin-ply composites, which are also an important aspect for aircraft operation. The projected damage area of the thin-ply laminates is reduced by 46% compared to laminates with thicker plies. The decrease in flexural strength is significantly smaller, too.

While there are studies on specialised use cases, there is a lack of research quantifying the advantages of thin-ply composite materials on the full-scale level of commercial aircraft structures. To the authors knowledge, the only study that pursues a similar objective has been presented by Lovejoy and Scotti [29]. Herein, potential benefits from the use of hybrid thin plies are evaluated for the upper cover of a semi-span test article under compression-after-impact requirements. Without accounting for other design constraints, weight savings of up to 13% are reported. The present study contributes to bridging this research gap by assessing the potential benefits for the generic wing structure of a conceptual mid-range aircraft under multiple constraints. The generation of quantitative data is essential to determine how benefits observed at the coupon level and other effects associated with the use of thin plies translate to full-scale structures. An in-house finite-element (FE) wing model generator [30], which is described in the following section, is used for this assessment. Increased manufacturing costs associated with the use of thinner plies are not taken into account in the scope of this paper due to a lack of information. This is also related to the fact that automatised manufacturing processes, i.e., automated fiber placement (AFP), still need to be adapted to thin-ply materials. The processing of thin plies poses additional challenges to AFP, e.g., because they are more sensitive to temperature and mechanical stress during layup [31] and minimisation of manufacturing-related defects such as gaps becomes more difficult [32]. The authors nevertheless acknowledge that e.g., halving the ply thickness doubles the layup area and would therefore inevitably raise production costs.

2. Methodology

2.1. Model Generation and Sizing

The parametric wing model generation process used in this study is shown schematically in Figure 1. It makes use of the parametric data format CPACS [33] (Common parametric aircraft configuration scheme) developed by the German Aerospace Centre DLR and the associated geometry library TiGL [34]. First, the wing's aerodynamic hull and basic structural elements—spars, ribs and stringers—are defined in a hierarchical CPACS XML file. TiGL is then used to generate the corresponding geometry and export it as STEP files, which are subsequently imported into Abaqus/CAE.

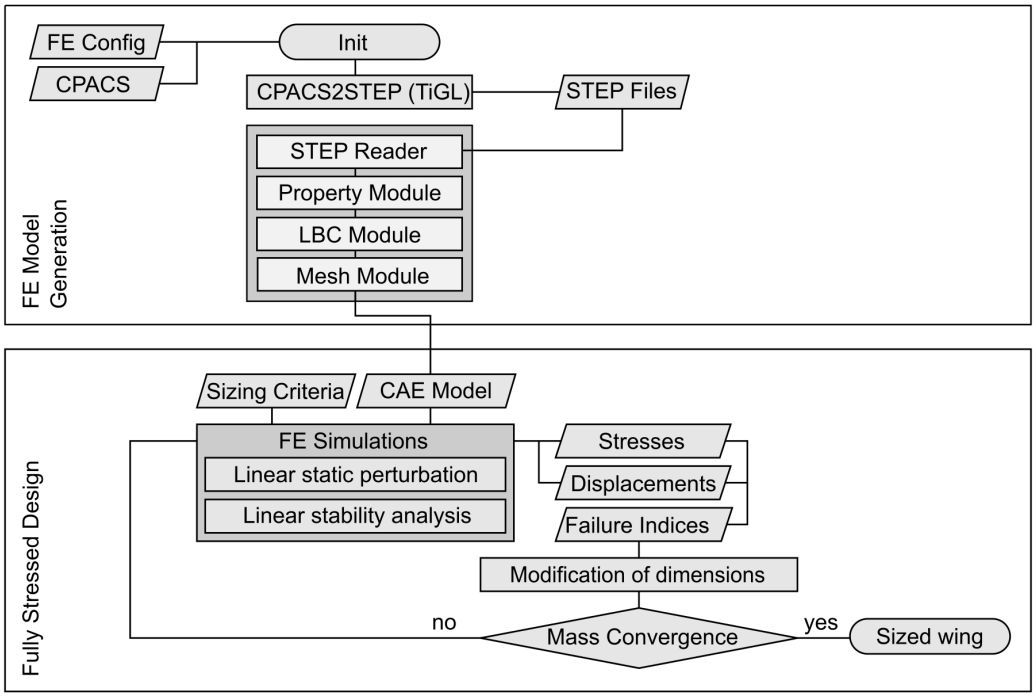

Figure 1. Flow chart of the model generation and sizing procedure.

In Abaqus/CAE, an automated process is executed based on a configuration file for the FE analysis. This process includes functionalities for the assignment of material properties, for connecting the individual parts, for meshing and for the application of loads and boundary conditions. Surfaces are modelled using shell elements, while stiffeners, such as stringers, spar caps and rib caps, are idealised using beam elements. This level of fidelity is commonly chosen for global wing models as a compromise between accuracy and modelling effort.

The FE wing model is sized using an iterative fully-stressed design (FSD) approach, comparable to Rieke [35] and Sommerwerk et al. [36]. Within each iteration, failure indices are calculated for all shells and stiffeners and for all sizing criteria, respectively. The indices are equal to 0.0 when the component is unloaded and equal to 1.0 when the loading is equivalent to the allowed maximum loading. The wall thickness of each shell and stiffener is adjusted based on its critical failure index at the end of each iteration. If the absolute change in total mass of the wing structure is lower than a defined limit in two consequetive iterations, the sizing is terminated. In this study, the limit is set to 0.5% of the total mass. The convergence behaviour of the FSD is influenced by various parameters such as the maximum wall thickness modification in between two iterations, damping and smoothing. The following settings have been chosen for this study:

$$t_{i+1} = \begin{cases} t_i \cdot \max\left(0.85,\, 0.99 \cdot \sqrt{FI_{Crit}}\right) & \text{if } FI_{Crit} < 0.95 \\ t_i & \text{if } 0.95 \leq FI_{Crit} \leq 1.0 \\ t_i \cdot \min\left(1.075,\, 1.01 + \sqrt{FI_{Crit}^2 - 1}\right) & \text{if } FI_{Crit} > 1.0 \end{cases} \quad (2)$$

The following analysis makes use of the failure criterion according to Puck [37] in order to assess the material's strength. Global linear stability analyses of the entire wing structure are used to assess buckling in an approach similar to Hürlimann et al. [38]. This global approach allows the consideration of unconventional panel geometries and provides a holistic view of the wing's stability behavior. However, buckling of structural components, i.e., shells and beam stiffeners, can influence the stability of others. While local buckling of

skin panels has to be prevented up to the limit load, global buckling has to be prevented up to the ultimate load. In previous studies, the stiffness of the composite layups in the global wing models has been smeared. However, smearing the laminate stiffness neglects the influence of D_{16} and D_{26} within the ABD matrix. The stability considerations discussed in the previous section therefore have to be assessed before analysing the other effects with global FE analysis, to evaluate whether this simplification remains valid.

As an enhancement to previous studies, the wall thickness adjustment routine has been modified to take into account the failure mode of the strength criterion according to Puck, which distinguishes fibre failure as well as different inter-fibre failures modes. If the failure index of a layer exceeds its allowable limit and fibre failure is the governing mode, it is meaningful to reinforce this very layer by increasing its wall thickness. If, however, an inter-fibre mode is critical, thickening the same layer will not reduce its failure index. Instead, depending on the stress state, the perpendicular and/or $\pm 45°$-rotated layers need to be reinforced.

The impact of an increase in strength on the mass of the different wing components and the total primary wing structure is analysed by running FSD simulations with different material properties. Regarding the extended design space of thin-ply composite materials, two aspects are covered in the scope of this paper: Similarly to the strength parameters, the minimum wall thickness is varied within FSD simulations to assess the fact that quasi-isotropic designs can be achieved with lower total laminate thickness. Additionally, a simple manufacturing constraint is applied subsequently to the FSD simulations to account for the reduced step size discussed in Section 1. Here, the required material in each direction is increased to the next highest multiple of the ply thickness. Benefits from the stability considerations are assessed separately in Section 2.4.

2.2. Validation of the Methodology Using a Simplified Wingbox Structure

The implemented methodology was validated using the academic example of a simplified wingbox structure, which has been defined by Liu et al. [39,40] and subsequently employed by various authors [41–43] as a benchmark. The structure is shown schematically in Figure 2. The rectangular wingbox consists of upper and lower skin as well as three ribs and four spars, which are arranged equidistantly. This results in nine skin panels on both the upper and lower skin. Only the layup of these skin panels is subject to the sizing and optimisation process. The ribs and spars are composed of $\pm 45°$ layers and remain unchanged during optimisation. The original model variant does not include any beam stiffening elements. It is clamped in the X–Z plane and loaded at the wing tip by four point loads that induce both bending and torsion. With the dimensions defined by Liu, the unstiffened skin panels are relatively large compared to typical wing structures. In all computations compared here, the material properties of T300/5208 are used. These properties are listed in Table 2.

Table 2. Material properties of T300/5208.

E_1/GPa	E_2/GPa	G_{12}/GPa	ν_{12}	$\rho/\frac{kg}{m^3}$	ϵ_1	ϵ_2	γ_{12}	X/MPa	Y/MPa	S/MPa
128.0	13.0	6.4	0.3	1578	0.008	0.029	0.015	1016.0	377.0	96.15

Liu et al. [39,40] propose a two-stage process for layup optimisation that accounts for both strength and stability criteria. At the global level, the design variables are the number of plies in the 0°-, 90°- and $\pm 45°$-directions. By assuming a symmetric and balanced laminate, there are three design variables per skin panel. Based on the ply share obtained from an optimisation at the global level, a discrete stacking sequence is optimised at skin

panel level to maximise buckling stiffness. In [44], Liu and Haftka introduce continuity constraints to increase the fraction of unidirectional plies that span adjacent skin panels and improve both the structural integrity at the panel transitions and the manufacturability of the wingbox. They perform trade-off studies between the degree of continuity and the resulting wing mass. Their results show that a continuity level of up to about 70% can be achieved with only a slight mass penalty, whereas higher continuity levels lead to a more pronounced increase in mass. Without any continuity constraints, the total mass is 228.9 kg. By enforcing 90% fiber continuity between adjacent skin panels, the mass increases to 265.6 kg. Seresta et al. [41] employ a guide-based approach to further enhance the degree of continuity: starting from a template stacking (guide), unidirectional plies are successively removed until a failure criterion is violated. They likewise generate discrete stacking sequences for the individual skin panels, composed of 0°-, 90°- and 45°-plies. Seresta et al. achieve full continuity at a total mass of about 232.8 kg. However, the lower wing skin is only checked against strength failure in their study. Buckling failure, which can still occur due to shear loading, is not considered here. Dähne et al. [43] use the model to validate the modular Lightworks simulation environment, which enables model creation at varying levels of complexity. For the unstiffened wingbox, they obtain a total mass of 226.2 kg. The numbers do only represent upper and lower skin mass.

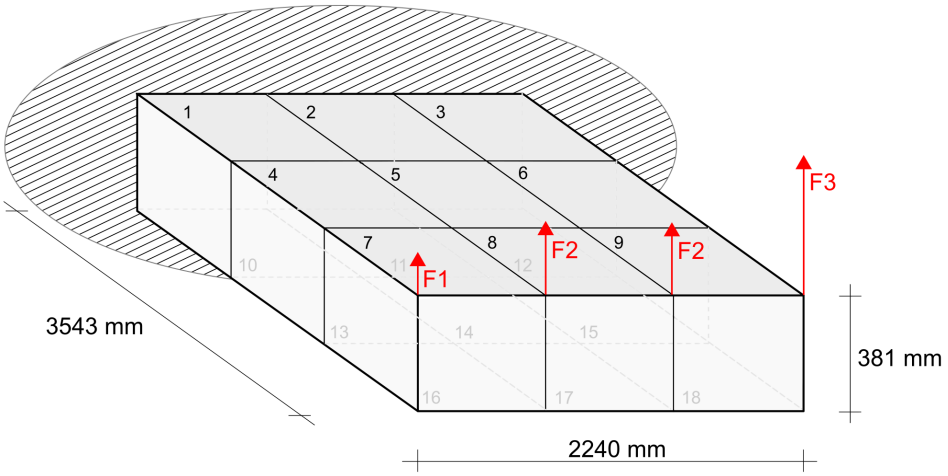

Figure 2. Academic wingbox structure used for validation purposes: dimensions, panel numbering and applied forces F_1 = 90 kN, F_2 = 187.9 kN and F_3 = 380.2 kN.

The wingbox model is well suited for validation purposes as it can be investigated with various methods at low effort. Nevertheless, methodological differences between the approaches can impose limitations on model comparability. In the present comparison, these differences primarily concern the stability analysis. Due to the global approach described above, buckling of ribs and spars can influence the stability of skin panels. Since these are disregarded in the other studies, the buckling stiffness of ribs and spars is increased artificially in this validation, by adding a foam core that doesn't significantly increase the bending stiffness of the global structure.

Figure 3 shows a comparison of the wall thickness distribution across the skin panels between literature and own FSD simulations, which result in a slightly conservative total mass of 254.82 kg (upper and lower skin). All authors' results agree well both qualitatively and quantitatively. Due to the large panel dimensions, the required thickness is substantially higher on the upper skin, which is driven by buckling constraints, than on the tension-loaded lower skin.

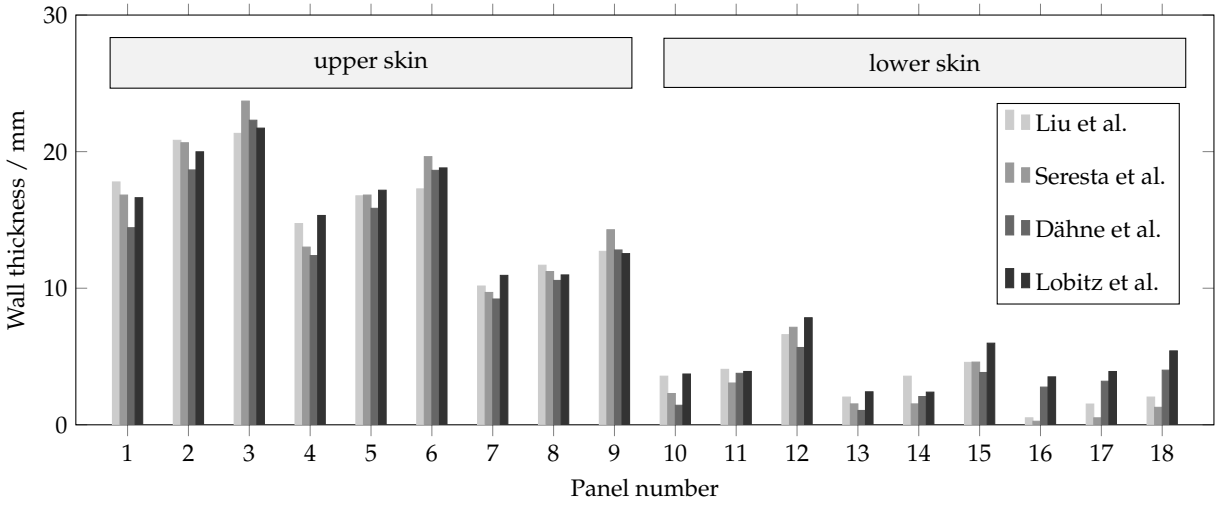

Figure 3. Comparison of the wall thickness across the upper (1–9) and lower (10–18) skin panels with literature results [40,41,43].

The FSD results from Figure 3 have been obtained with an approximate element edge length of 100 mm and a uniform initial thickness distribution. Since element size and start design may influence the results of the FSD, Figures 4 and 5 illustrate the convergence behaviour with respect to element size the robustness with respect to different start designs. The following parameters have been varied within the start designs:

- Initial skin thickness ranging from 2 mm to 30 mm and representing both under- and oversized start designs;
- Spanwise variation of the initial skin thickness, with the thickness either increasing or decreasing with span (each pattern applied once in a moderate and in a stronger form).

While an extremely coarse mesh significantly overestimates the buckling stiffness, the difference between 75 mm and 200 mm approximate element edge length remains below 5%. With a standard deviation of less than 2 kg, the difference due to the modified start design is negligible for the test cases.

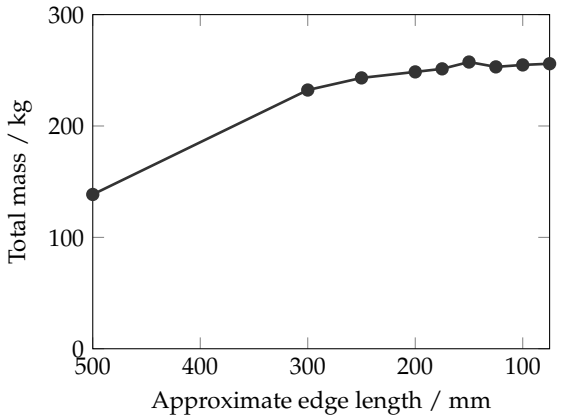

Figure 4. Mesh convergence of the FSD for the academic wingbox.

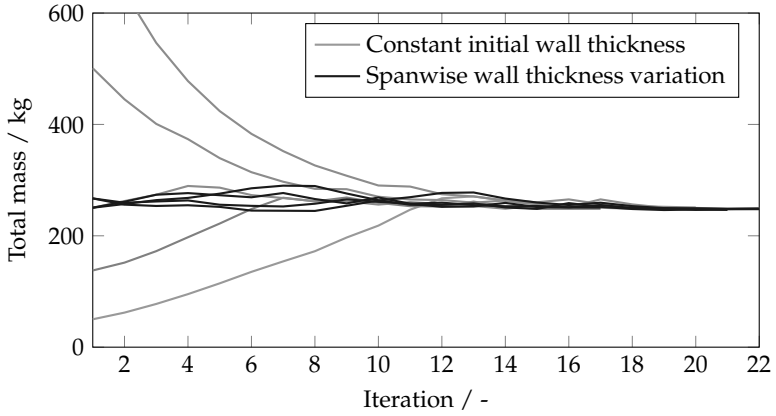

Figure 5. Mass convergence of the FSD for the academic wingbox with an approximate edge length of 100 mm and different start designs.

2.3. Use Case for the Assessment of Thin-Ply Materials

The conceptual design of a medium-range aircraft [3] developed within the framework of SE^{2}A is used to analyse the different potential benefits. A rendering of the aircraft is shown in Figure 6. The design range is 4000 km with a maximum payload of 19,650 kg. In order to minimise the climate impact of the aircraft in operation, the design adheres to the "lower and slower" principle. The cruise Mach number is 0.71 and the cruise altitude is 7650 m. The cruise altitude is a compromise between the fact that the climate impact, especially with respect to contrails, significantly increases with altitude and the need to fly above mid-level clouds. The cruise Mach number has to be reduced subsequently to maintain maximum aerodynamic efficiency.

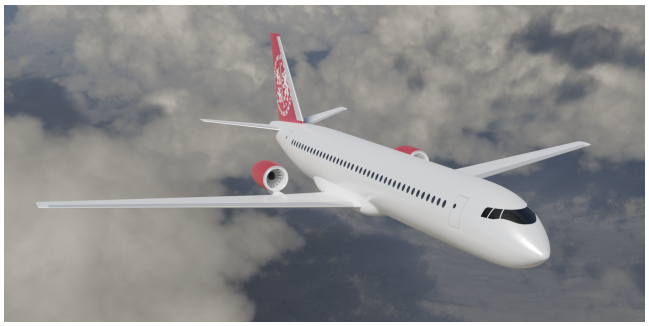

Figure 6. Rendering of the medium-range aircraft configuration of SE^{2}A.

In this study, the generic wing structure shown in Figure 7 is defined in accordance to typical wingbox designs [45]. The spars are located at 20.0% and 62.5% of the chordlength, the nominal stringer pitch is set to 200 mm and the rib spacing is set to 500 mm. The laminate of the wing covers is oriented in the direction of the stringers with an angle of 12° from the global y-axis. IM6EP is chosen as the material for the composite layup. Stiffeners are modelled as beam elements with smeared properties containing 60% 0°-layers, 30% 45°-layers and 10% 90°-layers. The properties of IM6EP are listed in Table 3. The aerodynamic loads have been calculated in the conceptual design for 2.5 g and −1.0 g load cases. Load alleviation from the mass of the engines and fuel is not accounted for in the scope of this paper.

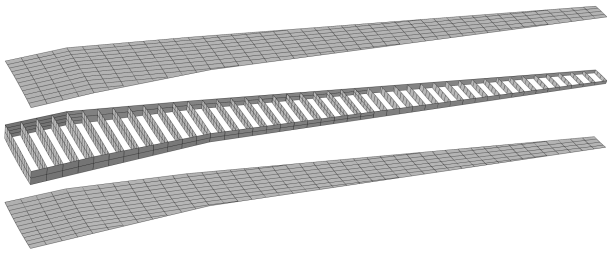

Figure 7. Structural model of the wingbox with upper skin (**top**), ribs and spars (**center**) and lower skin (**bottom**).

Table 3. Material properties of IM6EP.

E_1/GPa	E_2/GPa	G_{12}/GPa	ν_{12}	$\rho/\frac{kg}{m^3}$	X_T/MPa	X_C/MPa	Y_T/MPa	Y_C/MPa	S/MPa
177.0	10.8	7.6	0.27	1600.0	2860.0	1875.0	49.0	246.0	83.0

2.4. Prestudy: Stability Considerations

In a prestudy, a simplified rectangular stiffened panel under compressional loading is used to estimate the influence of the ply thickness on the buckling stability (see Figure 8). In accordance to Section 2.3, the dimensions are 500 mm × 200 mm and IM6EP is used as the material. The total laminate thickness ranges from 1 mm to 6 mm with the ply thickness varying in physically meaningful limits from 0.04 mm (thin plies) to 0.25 mm (thick plies) in a QI stacking. The resulting buckling load obtained from FE-based linear stability analysis conducted in Abaqus is standardised with the one of a ply thickness of 0.125 mm to illustrate the effect. The comparison also includes an idealised laminate (*inf.*), in which the coupling coefficients D_{16} and D_{26} are neglected.

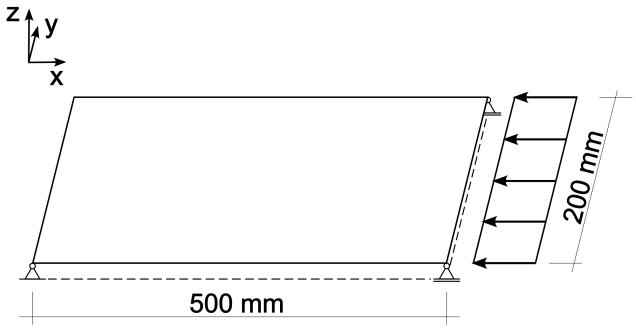

Figure 8. Simplified rectangular stiffened panel used to estimate influence of ply thickness on buckling stability.

The results, which are shown in Figure 9, indicate that the use of thin plies only results in a significantly improved stability for laminates with a rather low total thickness. The potential improvement for a laminate with a total thickness of 1 mm is 26% in comparison to standard plies. For thinner laminates, which are, however, not manufacturable with standard plies and a QI stacking, the effect could further increase to some extent. Nevertheless, the improvement in buckling strength does not proportionally translate into weight savings since the buckling stiffness scales with the cube of the thickness (t^3). Therefore, in this case, the mass savings would rather amount to around 8.0%. For a laminate with a total thickness of 2.0 mm, the benefits are already negligible. Here, only a disadvantage from thick plies can be observed in contrast to standard ply thickness. With a total laminate thickness of 4.0 mm or higher, no relevant influence of the ply thickness on the buckling stability can be observed in the realistic range. Since only a small portion of the stiffened

panels within the wing structure may have such a thin layup, which is also constrained by other sizing criteria such as impact loads or repairability, the expected benefits from the stability considerations are assumed negligible for QI laminates at global wing level. It has therefore been chosen to smear the stiffness of the composite layup in this investigation to balance modelling effort and accuracy.

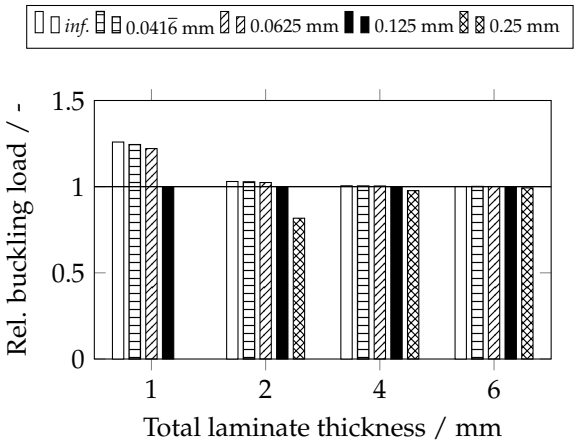

Figure 9. Standardised buckling load with different ply- and total laminate thickness. *inf.* refers to an infinitesimal ply thickness ($D_{16} = D_{26} = 0$)

3. Analysis on Global Wing Level

In order to quantify the expected mass reduction due to the different effects on the global wing level, a parameter study is performed under consideration of the literature review. In a full-factorial design of experiments the strength is modified in three steps: the original material parameters ($IM6EP_{orig}$), an increase in strength of 10% ($IM6EP_{10}$) and an increase in strength of 20% ($IM6EP_{20}$). Additionally, the minimum wall thickness is varied between 2.4 mm, 2.0 mm, 1.6 mm and 1.2 mm. A quasi-isotropic initial wall thickness of 5.0 mm is used for the whole wing structure in the initialisation of the FSD process.

Figure 10 illustrates the influence of an increase of the strength parameters and a modification of the minimum wall thickness on the total mass of the primary wing structure. In addition, Table 4 gives more detailed information on the composition of the total mass in the different FSD results. It is notable that the mass of the lower skin is significantly higher than the mass of the upper skin, which is surprising considering the facts that the tensile strength of IM6EP in fibre direction is more than 50% higher than the compressive one (see Table 3) and the upper skin is also prone to buckling. The reason for this development is the extremely low tensile strength of IM6EP perpendicular to the fibre direction. With the given material properties, the wall thickness on the lower cover is rather driven by inter-fibre failure in the 90°-layers than by fibre failure in the 0°-layers.

Table 4. Effect of strength improvements on mass of wing structure. Δm_{10} is defined as $(IM6EP_{10}/IM6EP_{Orig}) - 1$. Δm_{20} is defined as: $(IM6EP_{20}/IM6EP_{Orig}) - 1$.

Minimum Wall Thickness	Component	Mass/kg	Δm_{10}/%	Δm_{20}/%
(**a**) 2.4 mm	Total	1522.1	−6.9	−10.7
	Lower skin	691.1	−8.4	−16.4
	Upper skin	475.9	−7.5	−5.3
	Spars	191.6	−5.8	−13.0
	Ribs	163.5	−0.1	0.2

Table 4. *Cont.*

Minimum Wall Thickness	Component	Mass/kg	Δm_{10}/%	Δm_{20}/%
(**b**) 2.0 mm	Total	1500.7	−7.5	−13.4
	Lower skin	692.9	−8.6	−16.3
	Upper skin	485.2	−7.6	−10.6
	Spars	193.0	−8.0	−19.5
	Ribs	129.6	0.0	0.4
(**c**) 1.6 mm	Total	1479.8	−7.9	−13.0
	Lower skin	693.3	−8.5	−15.8
	Upper skin	491.1	−8.2	−10.5
	Spars	195.4	−9.7	−17.3
	Ribs	100.0	0.5	1.6
(**d**) 1.2 mm	Total	1475.7	−6.5	−12.5
	Lower skin	695.0	−8.1	−15.6
	Upper skin	492.4	−4.9	−4.0
	Spars	207.0	−10.1	−26.9
	Ribs	81.2	7.1	−0.4

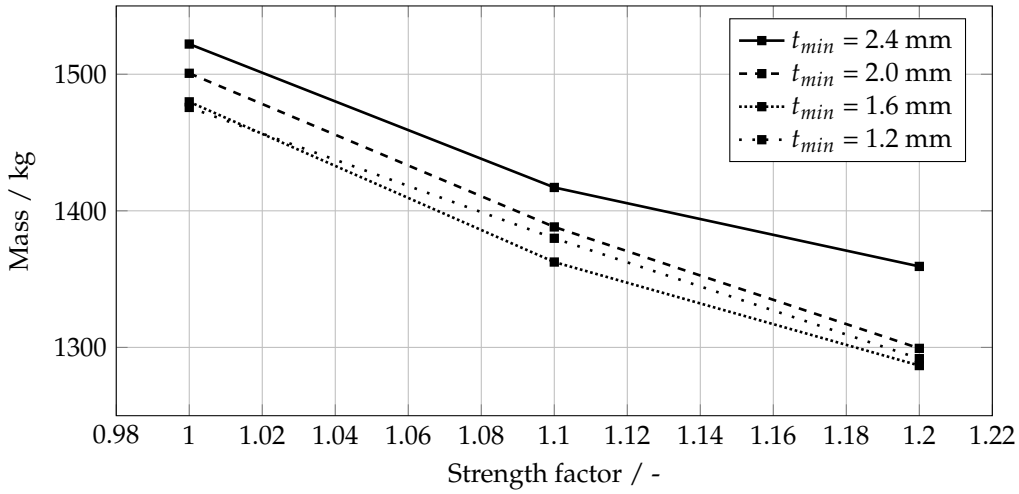

Figure 10. Resulting total mass with modified strength and minimum wall thickness. The strength factor is applied equally to all strength parameters.

3.1. Advantages from Increased Strength

Table 4 also contains more detailed information on the mass reduction due to the increased strength both for the total mass and the contribution of the different components. As Figure 10 already shows, the mass reduction consistently exhibits a slightly degressive course with respect to the increased strength for all the analysed variations in minimum wall thickness. For an increase in strength of 10%, the reduction in total mass is between 6.5% and 7.9%; for an increase in strength of 20% the resulting total mass is in total reduced by 10.7% to 13.4%. This order of magnitude seems reasonable since areas sized by strength requirements are expected to profit proportionally from the increased strength, while areas sized by other constraints are expected to profit less and areas sized by minimum wall thickness constraints do not profit from an increased strength at all.

A closer look at the different components reveals the origins of the mass reduction due to the increased strength. Figure 11 supports this discussion by illustrating the wall thickness distribution with respect to the strength and the decisive sizing criteria for a representative minimum wall thickness of 2.0 mm. The mean mass reduction in the lower skin is 8.4% for $IM6EP_{10}$ and 16.0% for $IM6EP_{20}$. As shown in Figure 11, the lower skin is mainly sized by strength requirements due to the tensional loads in the 2.5 g load case.

Only at the wing tip, the minimum wall thickness constraint governs the wall thickness. The slightly degressive behaviour of the mass reduction lies within the expected accuracy of the FSD approach, which not necessarily converges in the global optimum. It is, however, plausible, since a higher strength in general leads to a higher number of panels sized by minimum wall thickness. The lower skin provides the largest absolute contribution to mass reduction due to increased strength.

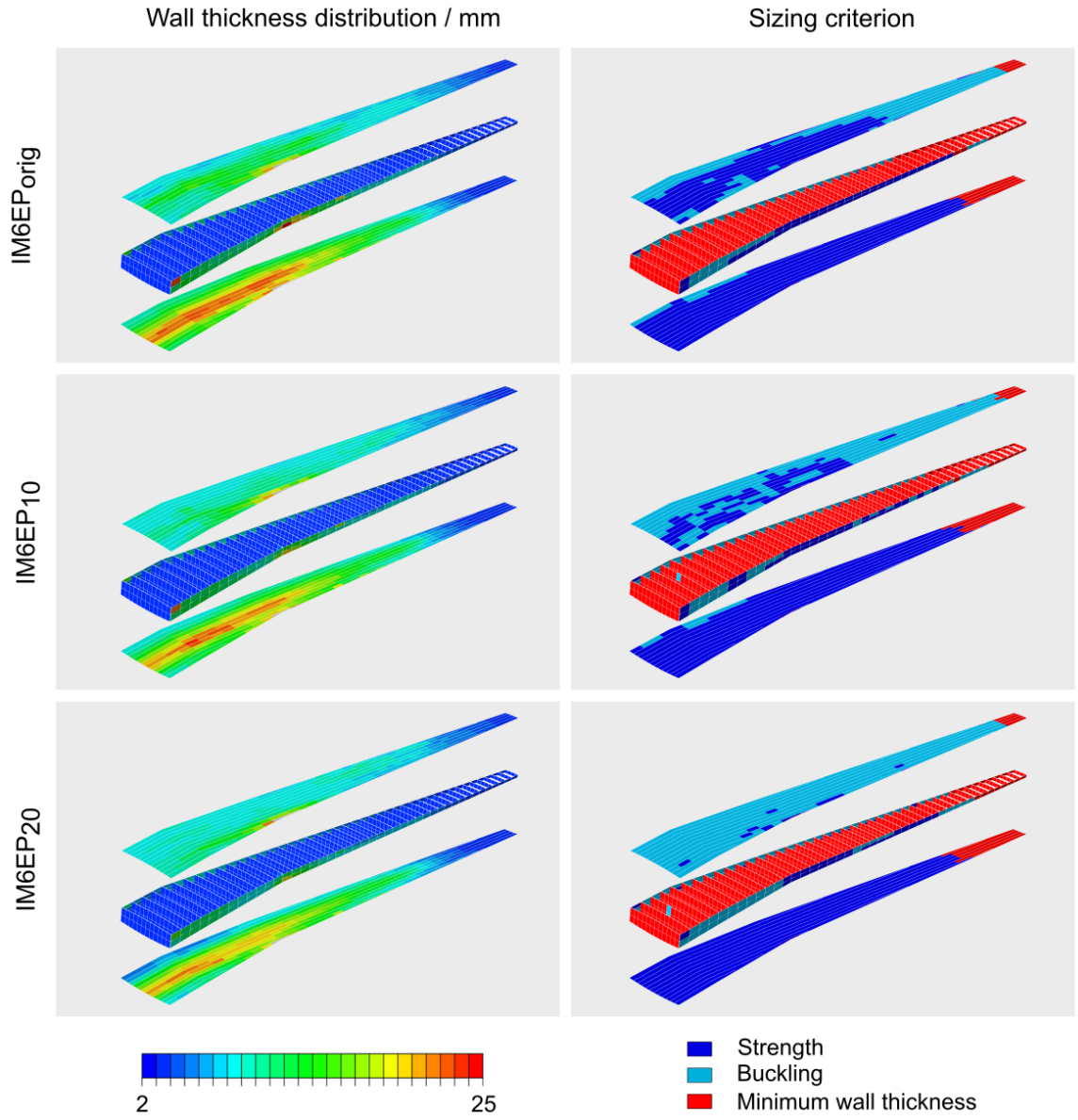

Figure 11. Wall thickness distribution and corresponding sizing criteria for wings with modified strength properties.

The mean mass reduction in the upper wing skin is 7.1% for $IM6EP_{10}$ but only 7.6% for $IM6EP_{20}$. Also the variance is considerably higher for $IM6EP_{20}$, with mass reduction ranging from only 4.0% to 10.6%. An explanation for the results may be found in Figure 11, too. With the given configuration, large parts of the upper skin, which are highly loaded, are sized by strength requirements with the original material parameters. Buckling becomes more critical also in these areas as the wall thickness decreases due to the increased strength. With $IM6EP_{20}$ only few skin panels remain sized by strength requirements in the upper skin. Therefore also the potential for mass reduction from strength improvement decreases. The increased variance in the sizings with different minimum wall thickness may be

attributed to the fact that the buckling criterion is more sensitive to variations then the strength criterion and the resulting designs therefore converge in different local optima.

The relative mass reduction of the spars shows a comparably high variance, too. This is, however, rather attributed to the fact, that the total mass is low compared to the mass of the wing covers, by which they are strongly influenced. e.g., the relative mass reduction of the spars with $IM6EP_{20}$ is very high (26.9%), while at the same time the mass reduction in the upper skin is very low, alleviating the loads in the spars.

The ribs are almost entirely sized by the minimum wall thickness constraint. Therefore, an increase in strength does not yield considerable benefits.

As stated in Section 2.3, a fixed stiffener layout is assumed in this study. As shown in Figure 11, the number of panels governed by buckling or strength requirements shifts due to the increase in strength with larger dimensions favoring buckling and smaller panels remaining strength-critical. Under the baseline material properties, large portions of the upper wing cover are sized by strength constraints, suggesting that the optimal stiffener spacing could be slightly larger. Nevertheless, the significant shift in sizing criteria of the upper skin for $IM6EP_{10}$ and $IM6EP_{20}$ indicates that the chosen layout is essentially balanced and close to the optimum. A moderate increase in stiffener spacing may diminish some of the gains from advanced materials and still yield slight overall savings in wing mass.

3.2. Advantages from Increased Design Freedom

Figure 10 already indicates that there is a measurable, but limited and degressive effect of the reduction in minimum wall thickness on the total mass of the primary wing structure. Table 5 shows the composition of the mass reductions exemplarily for $IM6EP_{orig}$. While there are small variation due to the nature of the FSD, the simulations with $IM6EP_{10}$ and $IM6EP_{20}$ yield similar results. The reduction clearly results from the total rib mass. For components sized by buckling, the reduced minimum wall thickness even leads to a slight increase in mass, which is attributed to a worse convergence behaviour within the FSD with such a low wall thickness. Even though the mass decrease within the ribs is very consistent, there are alternative measures for reducing their mass. In contrast to components which form the aerodynamic hull of the wing, ribs are well suited for topology optimisation [46]. The method has for instance been applied successfully to the ribs of the Airbus A380 [47]. While topology optimisation is most often used for isotropic materials, approaches for composite materials have also been developed (e.g., [48]). In the simulations presented here, the loads on the ribs are relatively low, maximising the benefits of relaxing the minimum wall thickness constraint. Topology optimisation is expected to yield similar improvements, eliminating the need for a costly use of thin-ply materials.

Table 5. Impact of variation in minimum wall thickness on mass of wing structure for $IM6EP_{orig}$.

Component	$m_{2.4mm}$/kg	$\Delta m_{2.0mm}$/%	$\Delta m_{1.6mm}$/%	$\Delta m_{1.2mm}$/%
Total	1522.1	−1.4	−2.8	−3.1
Lower skin	691.1	0.3	0.3	0.6
Upper skin	475.9	2.0	3.2	3.5
Spars	191.6	0.8	2.0	8.1
Ribs	163.5	−20.8	−38.9	−50.3

The analysis of the relatively simplistic manufacturing constraint described in Section 2.1 is illustrated in Figure 12. For all twelve FSD simulations, the wall thickness of each panel is increased to the next multitude of the ply thickness. The box plots show the statistically distributed influence of the application of the manufacturing constraint on the total mass of the primary wing structure. While the mass penalty is low

for thin plies with a thickness of 0.05 mm, it is already 5.4% in average for a ply thickness of 0.125 mm. For relatively thick plies (above 0.175 mm), the mass penalty in some cases even exceeds 10%. The results confirm the hypothesis that thin-ply composite materials also offer a significant potential for mass reduction due to the possibility of manufacturing smoother steps in the thickness distribution of symmetrical and balanced laminates. It may be promising to explore the applicability of hybrid laminates, comprising of layers with different ply thickness, to mitigate this penalty while avoiding the manufacturing effort of an all-thin-ply structure.

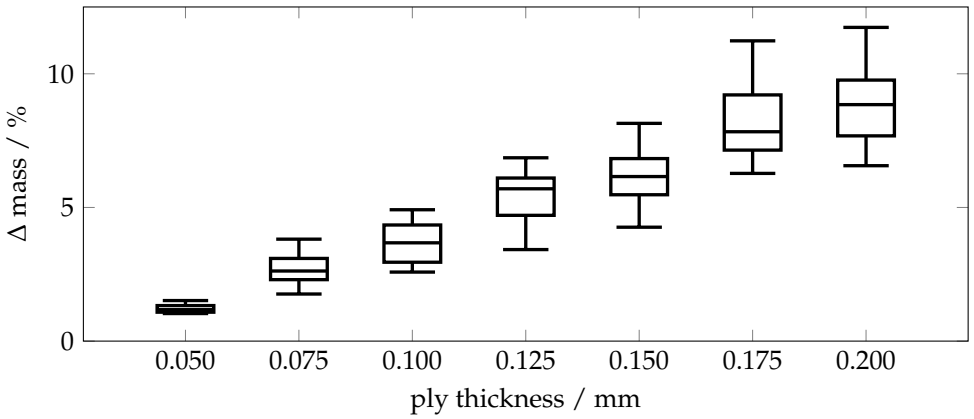

Figure 12. Additional mass with respect to ply thickness due to application of manufacturing constraint.

4. Conclusions

This paper assesses the application of thin-ply composite material in a conceptual mid-range aircraft wing. Potential advantages due to enhanced strength, an extended design space and improved buckling resistance are identified and evaluated based on FE simulations. The largest mass reduction due to the increased strength is found in the lower wing skin, which is the expected result given the predominant tensile loading under 2.5 g load cases. With increased strength properties, more areas of the upper wing skin become buckling-controlled, limiting the net benefit of the improved strength. A reduction of the minimum wall thickness is considered possible with the use of thin-ply composite materials as more layers with different orientation can be placed in a laminate of given total thickness. The extended design space in this regard only significantly affects the mass of the ribs in this study. There are, however, other options like topology optimisation to reduce the mass of the ribs as well, without requiring such high-performance materials as thin-ply composites. The manufacturing constraint discussed in Section 3.2 adds a significant mass penalty to wings made from thick plies, which can effectively be reduced with the employment of thin-plies. Here, the use of hybrid laminates consisting of plies with different thickness may be a suitable compromise balancing mass and manufacturing effort. Significant benefits from improved buckling stiffness have not been found.

In accordance to extensive experimental results on coupon level, significant benefits from the use of thin-ply composites materials are to be expected also on global wing level. Even though more sophisticated models covering a wider range of design constrains and load cases could refine the predictions, the present study gives quantitative indications on the net benefits on global wing level.

Previous applications of thin-ply composite materials in flying structures [24–26] are manually manufactured prototypes. For commercial use, only automatised manufacturing will result in a widespread use of thin plies at acceptable costs. Future research must therefore focus on adapting manufacturing processes to the unique requirements of thin-

ply composites for overcoming manufacturing related difficulties [31,32] and enabling their adoption in commercial aircraft structures.

Author Contributions: Conceptualization, L.L., C.B. and P.H.; methodology, L.L. and P.H.; writing—original draft preparation, L.L., C.B. and P.H.; writing—review and editing, L.L. and S.H.; supervision, S.H. and P.H.; project administration, S.H. and P.H.; funding acquisition, S.H. and P.H. All authors have read and agreed to the published version of the manuscript.

Funding: The authors would like to acknowledge the funding by the Deutsche Forschungsgemeinschaft (DFG, German Research Foundation) under Germany's Excellence Strategy-EXC 2163/1-Sustainable and Energy Efficient Aviation-Project-ID 390881007 as well as the support of the Ministry for Science and Culture of Lower Saxony (Grant No. ZN3945) for funding the research project "SaReMO - Safety, Resilience and Maintenance, Repair & Overhaul of Future Aviation Systems" in the initiative "ExzellenzStärken". The APC was funded by the TU Braunschweig Open Access Publication Fund.

Data Availability Statement: The data presented in this study is available on request from the corresponding author.

Conflicts of Interest: The authors declare no conflicts of interest. The funders had no role in the design of the study; in the collection, analyses, or interpretation of data; in the writing of the manuscript; or in the decision to publish the results.

Abbreviations

The following abbreviations are used in this manuscript:

CFRP	Carbon fibre-reinforced polymer
CPACS	Common parametric aircraft configuration schema
FE	Finite-element
FSD	Fully-stressed design
OHC	Open hole compression
OHT	Open hole tension
QI	Quasi-isotropic
SE^2A	Cluster of Excellence for Sustainable and Energy-Efficient Aviation

References

1. Beck, N.; Landa, T.; Seitz, A.; Boermans, L.; Liu, Y.; Radespiel, R. Drag reduction by laminar flow control. *Energies* **2018**, *11*, 252. [CrossRef]
2. Karpuk, S.; Elham, A. Influence of novel airframe technologies on the feasibility of fully-electric regional aviation. *Aerospace* **2021**, *8*, 163. [CrossRef]
3. Karpuk, S.; Radespiel, R.; Elham, A. Assessment of future airframe and propulsion technologies on sustainability of next-generation mid-range aircraft. *Aerospace* **2022**, *9*, 279. [CrossRef]
4. Galos, J. Thin-ply composite laminates: A review. *Compos. Struct.* **2020**, *236*, 111920. [CrossRef]
5. Sasayama, H.; Kawabe, K.; Tomoda, S.; Ohsawa, I.; Kageyama, K.; Ogata, N. Effect of Lamina Thickness on First Ply Failure in Multidirectionally Laminated Composites. *J. Jpn. Soc. Compos. Mater.* **2004**, *30*, 142–148. [CrossRef]
6. Kawabe, K.; Tomoda, S.; Matsuo, T. A pneumatic process for spreading reinforcing fiber tow. *Evol. Technol. Compet. Edge.* **1997**, *42*, 65–76.
7. Tsai, S.; Sihn, S.; Kim, R. Thin Ply Composites. In Proceedings of the 46th AIAA/ASME/ASCE/AHS/ASC Structures, Structural Dynamics and Materials Conference, Austin, TX, USA, 18–21 April 2005; AIAA: Reston, VA, USA, 2005. [CrossRef]
8. Sihn, S.; Kim, R.; Kawabe, K.; Tsai, S. Experimental studies of thin-ply laminated composites. *Compos. Sci. Technol.* **2007**, *67*, 996–1008. [CrossRef]
9. Yokozeki, T.; Aoki, Y.; Ogasawara, T. Experimental characterization of strength and damage resistance properties of thin-ply carbon fiber/toughened epoxy laminates. *Compos. Struct.* **2008**, *82*, 382–389. [CrossRef]
10. Arteiro, A.; Catalanotti, G.; Xavier, J.; Camanho, P. Notched response of non-crimp fabric thin-ply laminates. *Compos. Sci. Technol.* **2013**, *79*, 97–114. [CrossRef]

11. Amacher, R.; Cugnoni, J.; Botsis, J.; Sorensen, L.; Smith, W.; Dransfeld, C. Thin ply composites: Experimental characterization and modeling of size-effects. *Compos. Sci. Technol.* **2014**, *101*, 121–132. [CrossRef]
12. Furtado, C.; Arteiro, A.; Catalanotti, G.; Xavier, J.; Camanho, P. Selective ply-level hybridisation for improved notched response of composite laminates. *Compos. Struct.* **2016**, *145*, 1–14. [CrossRef]
13. Sebaey, T.; Mahdi, E. Using thin-plies to improve the damage resistance and tolerance of aeronautical CFRP composites. *Compos. Part A Appl. Sci. Manuf.* **2016**, *86*, 31–38. [CrossRef]
14. Wagih, A.; Maimí, P.; González, E.; Blanco, N.; de Aja, J.S.; de la Escalera, F.; Olsson, R.; Alvarez, E. Damage sequence in thin-ply composite laminates under out-of-plane loading. *Compos. Part A Appl. Sci. Manuf.* **2016**, *87*, 66–77. [CrossRef]
15. Cugnoni, J.; Amacher, R.; Kohler, S.; Brunner, J.; Kramer, E.; Dransfeld, C.; Smith, W.; Scobbie, K.; Sorensen, L.; Botsis, J. Towards aerospace grade thin-ply composites: Effect of ply thickness, fibre, matrix and interlayer toughening on strength and damage tolerance. *Compos. Sci. Technol.* **2018**, *168*, 467–477. [CrossRef]
16. Arteiro, A.; Furtado, C.; Catalanotti, G.; Linde, P.; Camanho, P. Thin-ply polymer composite materials: A review. *Compos. Part A Appl. Sci. Manuf.* **2020**, *132*, 105777. [CrossRef]
17. Arteiro, A. Structural Mechanics of Thin-Ply Laminated Composites. Ph.D. Thesis, University of Porto, Porto, Portugal, 2016.
18. Camanho, P.; Dávila, C.; Pinho, S.; Iannucci, L.; Robinson, P. Prediction of in situ strengths and matrix cracking in composites under transverse tension and in-plane shear. *Compos. Part A Appl. Sci. Manuf.* **2006**, *37*, 165–176. [CrossRef]
19. Moon, J.B.; Kim, M.G.; Kim, C.G.; Bhowmik, S. Improvement of tensile properties of CFRP composites under LEO space environment by applying MWNTs and thin-ply. *Compos. Part A Appl. Sci. Manuf.* **2011**, *42*, 694–701. [CrossRef]
20. Lovejoy, A.; Scotti, S.; Miller, S.; Heimann, P.; Miller, S. Characterization of IM7/8552 Thin-ply and Hybrid Thin-ply Composites. In Proceedings of the AIAA Scitech 2019 Forum, San Diego, CA, USA, 7–11 January 2019; AIAA: Reston, VA, USA, 2019. [CrossRef]
21. Kawabe, K.; Sasayama, H.; Kageyama, K.; Ogata, N. Effect of Ply Thickness on Compressive Properties in Multidirectionally Laminated Composites. *J. Jpn. Soc. Compos. Mater.* **2008**, *34*, 173–181. [CrossRef]
22. Masania, K.; Geissberger, R.; Stefaniak, D.; Dransfeld, C. Steel foil reinforced composites: Study of strength, plasticity and ply size effects. In Proceedings of the 20th International Conference on Composite Materials, Copenhagen, Denmark, 19–24 July 2015; ICCM: Montreal, Canada , 2015.
23. Huang, C.; He, M.; He, Y.; Xiao, J.; Zhang, J.; Ju, S.; Dazhi.; Xiaofei, J. Mechanical behaviors of thin-ply composite laminates under short-beam shear and open-hole tensile-loads: Pseudo-homogeneous and isotropic behaviors. In Proceedings of the 21th International Conference on Composite Materials, Xi'an, China, 20–25 August 2017; ICCM: Montreal, Canada, 2017.
24. Richardson, M. *Travelling Light*; Aerospace Manufacturing Magazine: Kent, UK, 2012; pp. 31–32.
25. Amacher, R.; Smith, W.; Dransfeld, C.; Botsis, J.; Cugnoni, J. Thin ply: From size-effect characterization to real life design. In Proceedings of the CAMX 2014—Composites and Advanced Materials Expo, Orlando, FL, USA, 13–16 October 2014; CAMX: Arlington, VA, USA, 2014.
26. Amacher, R.; Smith, W.; Botsis, J.; Dransfeld, C.; Cugnoni, J. New design opportunities using thin-ply composites. *JEC Compos. Mag.* **2015**, *52*, 33–35.
27. Yamashita, S.; Sonehara, T.; Takahashi, J.; Kawabe, K.; Murakami, T. Effect of thin-ply on damage behaviour of continuous and discontinuous carbon fibre reinforced thermoplastics subjected to simulated lightning strike. *Compos. Part A Appl. Sci. Manuf.* **2017**, *95*, 132–140. [CrossRef]
28. Yamashita, S.; Hirano, Y.; Sonehara, T.; Takahashi, J.; Kawabe, K.; Murakami, T. Residual mechanical properties of carbon fibre reinforced thermoplastics with thin-ply prepreg after simulated lightning strike. *Compos. Part A Appl. Sci. Manuf.* **2017**, *101*, 185–194. [CrossRef]
29. Lovejoy, A.E.; Scotti, S. Potential Weight Benefits of IM7/8552 Hybrid Thin-ply Composites for Aircraft Structures. In Proceedings of the AIAA Scitech 2019 Forum, San Diego, CA, USA, 7–11 January 2019; American Institute of Aeronautics and Astronautics: Reston, VA, USA, 2019. [CrossRef]
30. Lobitz, L.; Traub, H.; Overbeck, M.; Bień, M.; Heimbs, S.; Hühne, C.; Friedrichs, J.; Horst, P. Aircraft Wing Design for Extended Hybrid Laminar Flow Control. *Aerospace* **2023**, *10*, 938. [CrossRef]
31. Harik, R.; Lovejoy, A.; Yokan, C.; Jegley, D. Thin-ply: Exploration and manufacturing with automated fiber placement. In Proceedings of the CAMX 2020—Composites and Advanced Materials Expo, Orlando, FL, USA, 20–24 September 2020.
32. Kermani, N.N.; Gargitter, V.; Simacek, P.; Advani, S.G. Gap filling mechanisms during the thin ply automated tape placement process. *Compos. Part A Appl. Sci. Manuf.* **2021**, *147*, 106454. [CrossRef]
33. Alder, M.; Moerland, E.; Jepsen, J.; Nagel, B. Recent advances in establishing a common language for aircraft design with CPACS. In Proceedings of the Aerospace Europe Conference, Bordeaux, France, 25–28 February 2020; EUCASS Association: Bruxelles, Belgium, 2020.
34. Siggel, M.; Kleinert, J.; Stollenwerk, T.; Maierl, R. TiGL: An open source computational geometry library for parametric aircraft design. *Math. Comput. Sci.* **2019**, *13*, 367–389. [CrossRef]

35. Rieke, J. Bewertung von CFK-Strukturen in Einem Multidisziplinären Entwurfsansatz für Verkehrsflugzeuge. Ph.D. Thesis, TU Braunschweig, Braunschweig, Germany, 2013.
36. Sommerwerk, K.; Krukow, I.; Haupt, M.; Dinkler, D. Investigation of aeroelastic effects of a circulation controlled wing. *J. Aircr.* **2016**, *53*, 1746–1756. [CrossRef]
37. Puck, A.; Schürmann, H. Failure analysis of FRP laminates by means of physically based phenomenological models. *Compos. Sci. Technol.* **2002**, *62*, 1633–1662. [CrossRef]
38. Hürlimann, F.; Kelm, R.; Dugas, M.; Oltmann, K.; Kress, G. Mass estimation of transport aircraft wingbox structures with a CAD/CAE-based multidisciplinary process. *Aerosp. Sci. Technol.* **2011**, *15*, 323–333. [CrossRef]
39. Liu, B.; Haftka, R.; Akgun, M. Composite wing structural optimization using genetic algorithms and response surfaces. In Proceedings of the 7th AIAA/USAF/NASA/ISSMO Symposium on Multidisciplinary Analysis and Optimization, St. Louis, MO, USA, 2–4 September 1998; p. 4854.
40. Liu, B.; Haftka, R.T.; Akgün, M.A. Two-level composite wing structural optimization using response surfaces. *Struct. Multidiscip. Optim.* **2000**, *20*, 87–96. [CrossRef]
41. Seresta, O.; Gürdal, Z.; Adams, D.B.; Watson, L.T. Optimal design of composite wing structures with blended laminates. *Compos. Part B Eng.* **2007**, *38*, 469–480. [CrossRef]
42. Scardaoni, M.P.; Montemurro, M. A general global-local modelling framework for the deterministic optimisation of composite structures. *Struct. Multidiscip. Optim.* **2020**, *62*, 1927–1949. [CrossRef]
43. Dähne, S.; Werthen, E.; Zerbst, D.; Tönjes, L.; Traub, H.; Hühne, C. Lightworks, a scientific research framework for the design of stiffened composite-panel structures using gradient-based optimization. *Struct. Multidiscip. Optim.* **2024**, *67*, 70. [CrossRef]
44. Liu, B.; Haftka, R. Composite wing structural design optimization with continuity constraints. In Proceedings of the 19th AIAA Applied Aerodynamics Conference, Anaheim, CA, USA, 11–14 June 2001; p. 1205.
45. Niu, M. *Airframe Structural Design: Practical Design Information and Data on Aircraft Structures*; Hong Kong Conmilit Press Ltd.: Hong Kong, China, 1988.
46. Zhu, J.; Zhang, W.; Xia, L. Topology optimization in aircraft and aerospace structures design. *Arch. Comput. Methods Eng.* **2016**, *23*, 595–622. [CrossRef]
47. Krog, L.; Tucker, A.; Kemp, M.; Boyd, R. Topology optimisation of aircraft wing box ribs. In Proceedings of the 10th AIAA/ISSMO Multidisciplinary Analysis and Optimization Conference, Albany, NY, USA, 30 August–1 September 2004; p. 4481.
48. Peeters, D.; van Baalen, D.; Abdallah, M. Combining topology and lamination parameter optimisation. *Struct. Multidiscip. Optim.* **2015**, *52*, 105–120. [CrossRef]